ADVANCES IN ATMOSPHERIC SCIENCES, VOL. 37, JUNE 2020, 569–575

• Original Paper •

Two-Year Observation of Fossil Fuel Carbon Dioxide Spatial Distribution in Xi'an City

Xiaohu XIONG*[1,2], Weijian ZHOU[1,2,3,4,5], Shugang WU[1,2], Peng CHENG[1,2], Hua DU[1,2], Yaoyao HOU[1,2], Zhenchuan NIU[1,2,4], Peng WANG[1,2], Xuefeng LU[1,2], and Yunchong FU[1,2]

[1]*State Key Laboratory of Loess and Quaternary Geology, Institute of Earth Environment, Chinese Academy of Sciences, Xi'an* 710061, *China*

[2]*Shaanxi Key Laboratory of AMS Technology and Application, Xi'an AMS Center, Xi'an* 710061, *China*

[3]*Xi'an Jiaotong University, Xi'an* 710049, *China*

[4]*Chinese Academy of Sciences Center for Excellence in Quaternary Science and Global Change, Xi'an* 710061, *China.*

[5]*Open Studio for Oceanic-Continental Climate and Environment Changes, Pilot National Laboratory for Marine Science and Technology (Qingdao), Qingdao* 266237, *China*

(Received 1 November 2019; revised 6 January 2020; accepted 9 January 2020)

ABSTRACT

The need for atmospheric carbon dioxide (CO_2) reduction in the context of global warming is widely acknowledged by the global scientific community. Fossil fuel CO_2 (CO_{2ff}) emissions occur mainly in cities, and can be monitored directly with radiocarbon (^{14}C). In this research, annual plants [*Setaria viridis* (L.) Beauv.] were collected from 26 sites in 2013 and 2014 in the central urban district of Xi'an City. The $\Delta^{14}C$ content of the samples were analyzed using a 3 MV Accelerator Mass Spectrometer, and CO_{2ff} concentrations were calculated based on mass balance equations. The results showed that the CO_{2ff} mixing ratio ranged from 15.9 to 25.0 ppm (part per million, equivalent to μmol mol^{-1}), with an average of 20.5 ppm in 2013. The range of measured values became larger in 2014, from 13.9 ppm to 33.1 ppm, with an average of 23.5 ppm. The differences among the average CO_{2ff} concentrations between the central area and outer urban areas were not statistically significant. Although the year-to-year variation of the CO_{2ff} concentration was significant ($P < 0.01$), there was a distinctly low CO_{2ff} value observed in the northeast corner of the city. CO_{2ff} emissions from vehicle exhaust and residential sources appeared to be more significant than two thermal power plants, according to our observed CO_{2ff} spatial distribution. The variation of pollution source transport recorded in our observations was likely controlled by southwesterly winds. These results could assist in the optimal placement of regional CO_2 monitoring stations, and benefit the local government in the implementation of efficient carbon emission reduction measures.

Key words: fossil fuel CO_2, ^{14}C, Xi'an, carbon emissions reduction, *Setaria viridis*

Citation: Xiong, X. H., and Coauthors, 2020: Two-year observation of fossil fuel carbon dioxide spatial distribution in Xi'an City. *Adv. Atmos. Sci.*, **37**(6), 569–575, https://doi.org/10.1007/s00376-020-9241-4.

Article Highlights:

- The spatial distribution of CO_{2ff} indicated by plant $\Delta^{14}C$ measurements in Xi'an is presented.
- The year-to-year variation of CO_{2ff} from different sites in Xi'an was significant.
- The northeast corner of Xi'an central area featured distinctly lower CO_{2ff} values.
- Vehicle exhaust emissions and residential emissions appeared to control the spatial differences.
- Weather conditions (wind direction in particular) also influenced regional temporal CO_{2ff} variations.

1. Introduction

Atmospheric carbon dioxide (CO_2) reached a new level in 2017 (405.5 ppm), equal to 146% of the pre-industrial level, and is mainly attributed to anthropogenic fossil fuel emissions (WMO, 2018). Global net anthropogenic CO_2 emissions should decline by about 45% from 2010 levels by 2030 to limit global warming to below 1.5°C (IPCC, 2018). Therefore, reliable methods to quantify anthropogenic CO_2 emissions are essential. Two methods have been commonly applied: "bottom-up" and "top-down." The former is based on activity data and emission factors (IPCC, 2006). The reliability of this method not only depends on the quality of statist-

* Corresponding author: Xiaohu XIONG
Email: xiongxh@ieecas.cn

ical activity data, but also on the accuracy of emission factors (Liu et al., 2015). The estimated uncertainty of the "bottom-up" method has been estimated to range from a few percent to about 50% on an individual national scale (Andres et al., 2012); and may be as high as 100% on an urban scale (Gurney et al., 2009; Peylin et al., 2011; Turnbull et al., 2011). The "top-down" method usually measures the atmospheric CO_2 mixing ratio from ground stations (Levin et al., 2003), aircraft (Turnbull et al., 2016) or satellites (Buchwitz et al., 2017). This approach can produce high temporal and spatial resolutions using CO_2 data. However, observed CO_2 fluctuations do not directly measure fossil fuel CO_2 (CO_{2ff}) emissions, as both CO_{2ff} and natural CO_2 (e.g., from heterotrophic respiration) can contribute to atmospheric CO_2 variations.

Radiocarbon (^{14}C) is a unique and powerful tracer for CO_{2ff} and a useful tool to verify "bottom-up" inventory estimates (Levin et al., 2003; Nisbet and Weiss, 2010; Turnbull et al., 2016). $\Delta^{14}C$ in plants has been widely used to represent mean daytime atmospheric $\Delta^{14}C$ during their growth period for quantification of atmospheric CO_{2ff} (e.g. Lichtfouse et al., 2005; Bozhinova et al., 2013; Turnbull et al., 2014). Plant samples are easier to collect in a large area at low cost, as compared with air samples (Turnbull et al., 2014), and are especially advantageous when focusing on the spatial distribution of CO_{2ff} (Hsueh et al., 2007; Riley et al., 2008). Cities, with concentrated carbon emissions and frequently affected by serious air pollution meanwhile, have been recognized as playing a key role in the action of climate change mitigation (Rosenzweig et al., 2010; Hoornweg et al., 2011). The spatial distribution of CO_{2ff} indicated by plants has been investigated in a few cities (Xi et al., 2011, 2013; Djuricin et al., 2012; Zhou et al., 2014; Beramendi-Orosco et al., 2015; Niu et al., 2016); however, very few city centers have been targeted, because of the lack of particular species (e.g., corn leaves were chosen in many studies) in city centers. Interannual CO_{2ff} variations and their spatial distribution based on plants is also scarce (Bozhinova et al., 2016). Green foxtail samples have been successfully used to reflect CO_{2ff} differences in some areas in Xi'an City in 2010 (Zhou et al., 2014). In this study, green foxtail was sampled across a wide distribution of sites in the central urban area of Xi'an in 2013 and 2014 to investigate the atmospheric CO_{2ff} spatial distribution and its year-to-year variation. These data were used to quantify the spatial distribution and to estimate the influencing factors. The main goal was to provide quantitative information that can be used to improve local carbon emission reduction measures.

2. Methods

2.1. *Study sites and materials*

Xi'an is a famous tourist city and a significant node city of "the Belt and Road" initiative in the west of China. Its resident population reached 10 million in 2018. This city experiences a semiarid continental monsoon climate, with a mean annual temperature of 13.0°C–13.7°C. The mean annual rainfall is 522.4–719.5 mm, with over 80% of the precipitation falling in May to October. The winds are characteristically mild in Xi'an, with a prevailing northeasterly wind direction.

Annual plant samples [green foxtail, *Setaria viridis* (L.) Beauv.] from 26 sites inside the Xi'an Bypass Highway were collected in parks or scenic spots in October of 2013 and 2014. The distribution of these sites is shown in Fig. 1. Green foxtail is a C4 plant species, widely distributed in the city green belt as weeds. Its growing period is April to September in Xi'an City; thus, it reflects average atmospheric CO_{2ff} in the late spring–summer–early autumn in general. Every location sample was mixed by two or three individual plants with seed maturation, and all of them grew in open areas with good ventilation, as far as possible from urban trunk roads. Plant materials were air-dried before pretreatment.

2.2. *Experiment*

The grass leaves were soaked with 1-mol L^{-1} hydrogen chloride at 70°C for 2 h to remove any adhering carbonate, then rinsed with deionized water until neutral, and dried at 60°C. The dry plant materials (4–5 mg) were mixed with copper oxide (~200 mg) in a quartz tube and combusted at 850°C for 2 h under vacuum (~100 Pa). Finally, the CO_2 was extracted using liquid nitrogen as a cryogen, and further purified with liquid nitrogen/alcohol (−75°C) to remove water. The purified CO_2 was reduced to graphite carbon using zinc as a reductant over an iron catalyst. The produced graphite was pressed into an aluminum holder and measured in a 3-MV Accelerator Mass Spectrometer (High Voltage Engineering Europa B.V.) at the Xi'an AMS Center. Oxalic acid-II (NIST SRM 4990c) and coal were used as reference and blank, respectively. The measurement precision of a single sample is about 3‰ (1σ).

The ^{14}C results were calculated as $\Delta^{14}C$ values, according to the equation (Stuiver and Polach, 1977)

$$\Delta^{14}C = \frac{(^{14}C/^{12}C)_{samp} - (^{14}C/^{12}C)_{ref}}{(^{14}C/^{12}C)_{ref}}, \quad (1)$$

where $(^{14}C/^{12}C)_{samp}$ is the $^{14}C/^{12}C$ ratio of samples corrected for radioactive decay and normalized to a $\delta^{13}C$ of −25‰, and $(^{14}C/^{12}C)_{ref}$ is the $^{14}C/^{12}C$ ratio of the reference standard.

2.3. *Calculation of CO_{2ff}*

Atmospheric CO_2 (C_{obs}) can be considered to consist of three sources: (1) background CO_2 (C_{bg}), (2) fossil fuel-derived CO_2 (C_{ff}), and (3) other CO_2 sources (C_{other}). According to mass balance:

$$C_{obs} = C_{bg} + C_{ff} + C_{other}, \quad (2)$$

$$C_{obs}\Delta^{14}C_{obs} = C_{bg}\Delta^{14}C_{bg} + C_{ff}\Delta^{14}C_{ff} + C_{other}\Delta^{14}C_{other}. \quad (3)$$

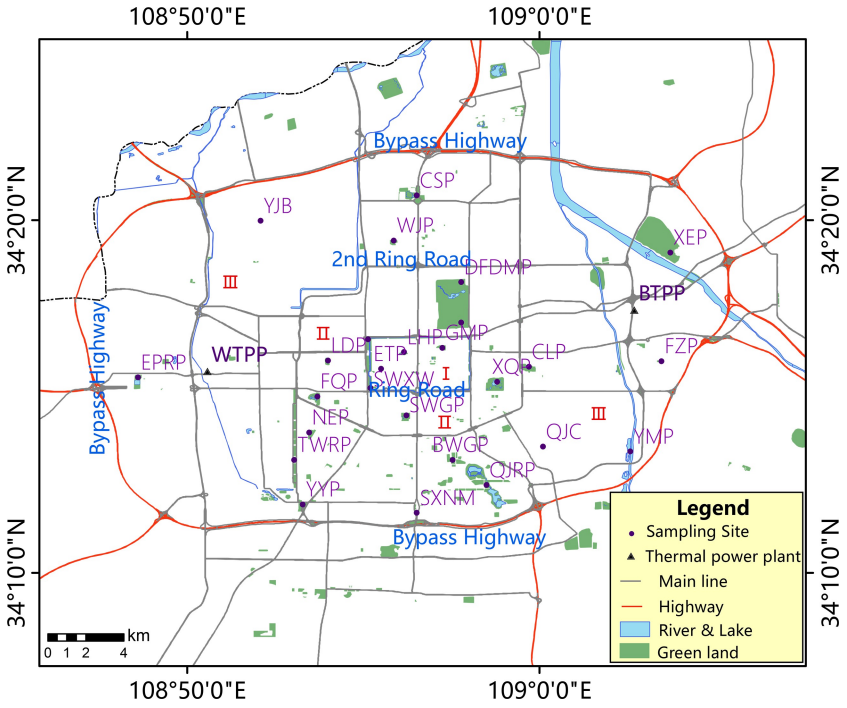

Fig. 1. The distribution of green foxtail sampling sites in the Xi'an urban area. Twenty-six sites (solid circles) were in the parks or in the scenic spots in the central urban district of Xi'an City. Two thermal power plants (solid triangles) were in the east and west area outside of the second Ring Road. The region inside the Bypass Highway was divided into three parts by the Ring Road and the second Ring Road, namely, Area I, II and III, respectively.

For time-integration, as in the case of seasonal plants, C_{obs} cannot be determined. Thus, Eq. (2) is substituted into Eq. (3), resulting in

$$C_{ff}=\frac{C_{bg}\left(\Delta^{14}C_{obs}-\Delta^{14}C_{bg}\right)}{\Delta^{14}C_{ff}-\Delta^{14}C_{obs}}-\frac{C_{other}\left(\Delta^{14}C_{other}-\Delta^{14}C_{obs}\right)}{\Delta^{14}C_{ff}-\Delta^{14}C_{obs}}. \quad (4)$$

The second term in this expression is usually omitted, because the error introduced is small (Turnbull et al., 2015). Equation (4) can then be simplified, and C_{ff} can be calculated by the following widely used formula:

$$C_{ff}=\frac{C_{bg}\left(\Delta^{14}C_{obs}-\Delta^{14}C_{bg}\right)}{\Delta^{14}C_{ff}-\Delta^{14}C_{obs}}. \quad (5)$$

In this equation, C_{ff} and C_{bg} are CO_2 derived from fossil fuel and CO_2 represented by background measurements, respectively; and $\Delta^{14}C_{obs}$ is measured in the plant samples. Because there is negligible ^{14}C in fossil fuel, the end-member value of $\Delta^{14}C_{ff} = -1000‰$ is assumed according to the definition of $\Delta^{14}C$ [Eq. (1)]. C_{bg} records were obtained from measurements made in the Mauna Loa Atmospheric Baseline Observatory in Hawaii, the United States (Tans and Keeling, 2019), and background $\Delta^{14}C$ data were from Jungfraujoch Atmospheric Baseline Observatory in Switzerland (Hammer and Levin, 2017).

3. Results and discussion

3.1. *Spatial variation of CO_{2ff} in 2013*

CO_{2ff} results from all sites in 2013 are shown in Fig. 2. The range of CO_{2ff} was 15.6–24.6 ppm, with an average of 20.1 ± 2.4 ppm. The average inside the Ring Road (5 sites, Area I), the Ring Road to the second Ring Road (6 sites, Area II) and the second Ring Road to the Bypass Highway segment (15 sites, Area III) were 19.8 ± 1.9 ppm, 19.6 ± 1.9 ppm and 20.4 ± 2.6 ppm, respectively. There were some sites with high CO_{2ff} values, such as the Southwest Xi'an City Wall (SWXW), Changle Park (CLP), Yongyang Park (YYP) and Yanming Park (YMP). These sites were scattered, but mainly located in the south of the Xi'an urban area. In contrast, sites with relatively low CO_{2ff} values were in the north, near the Bypass Highway. For example, the City Sports Park (CSP), Yuanjiabu Village (YJB), Xi'an World Horticulture Exposition Park (XEP), and the Epang Palace Relic Park (EPRP).

3.2. *Spatial variation of CO_{2ff} in 2014*

The spatial variations of CO_{2ff} in 2014 are shown in Fig. 3. In 2014, the average CO_{2ff} of all sites was 22.1 ± 5.4 ppm. The highest CO_{2ff} value was 31.7 ± 1.5 ppm, and the lowest was 12.5 ± 1.5 ppm. The average CO_{2ff} values of the above-mentioned three regions divided by the city's ring roads were 22.9 ± 5.5 ppm, 20.1 ± 2.5 ppm and 22.7 ± 6.1 ppm, respectively, without statistically significant differ-

ences. As shown in Fig. 3, both of the higher, and lower, CO_{2ff} values existed in the region inside the Ring Road, with a similar pattern within the second Ring Road to Bypass Highway area. It is interesting to note that the sites with higher CO_{2ff} values were widely distributed in the area adjacent the Bypass Highway, except for the northeast corner, with the two lowest values (City Sports Park and Xi'an World Horticulture Exposition Park).

3.3. *CO_{2ff} variation from 2013 to 2014*

A comparison of both years showed that CO_{2ff} variation in 2014 was larger than in 2013; the variation coefficients were 24% and 12%, respectively. Moreover, the differences between 2013 and 2014 were statistically significant

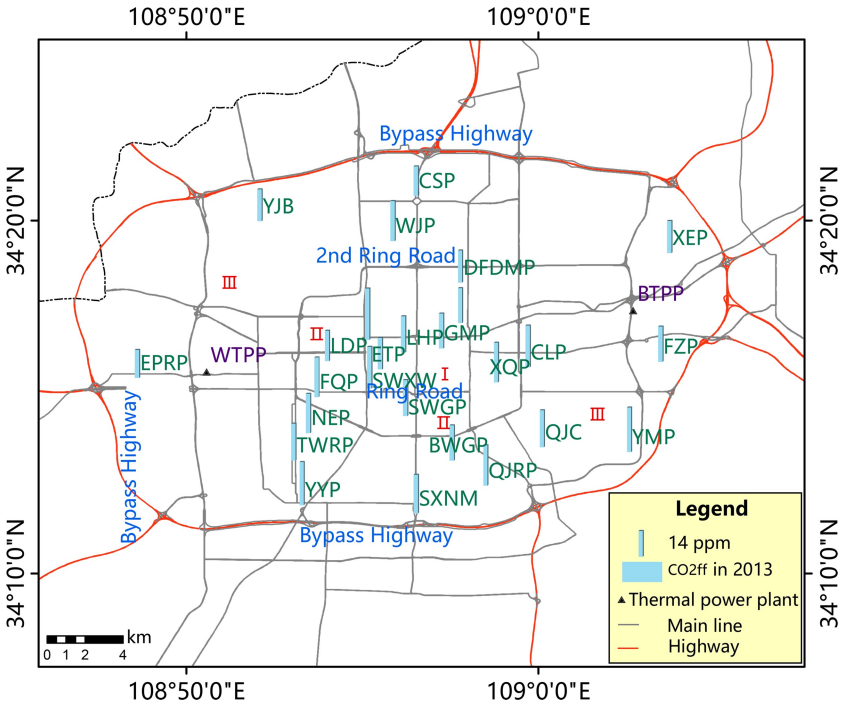

Fig. 2. CO_{2ff} mixing ratio spatial distribution in 2013. The value of CO_{2ff} is proportional to the height of the light blue column.

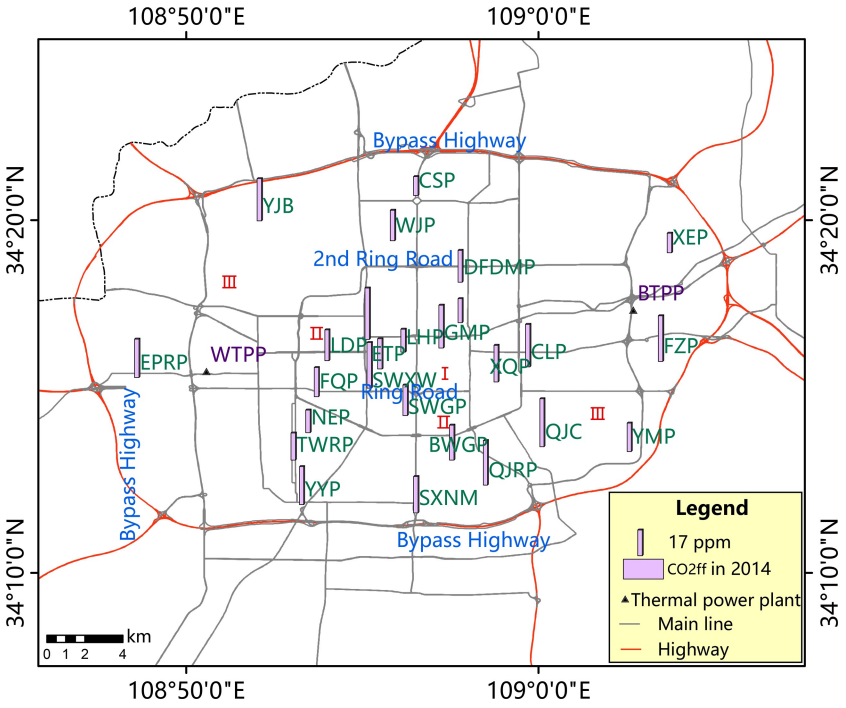

Fig. 3. CO_{2ff} mixing ratio spatial distribution in 2014. The value of CO_{2ff} is proportional to the height of the pink column.

($P < 0.01$, paired t-test) (Fig. 4). In detail, CO_{2ff} values at eleven sites increased from 2013 to 2014, and six decreased. Only nine sites showed minor changes. CO_{2ff} variations in Area II sites were smaller than observed for the other two areas. It is worth noting that most sites close to the Bypass Highway showed obvious increases, with two exceptional cases in the northeast: the City Sports Park and Xi'an World Horticulture Exposition Park. Further, CO_{2ff} from these two sites had the lowest values observed in both 2013 and 2014.

3.4. *CO_{2ff} differences between Chinese cities*

The CO_{2ff} mixing ratio was about 10–30 ppm in the Xi'an central urban district in 2013 and 2014, similar to that reported for 2010 (Zhou et al., 2014), and very close to downtown Beijing in 2009 (Niu et al., 2016). However, the Xi'an value was higher than that observed in some small and medium-sized cities (e.g., Lhasa, Jiuquan, Erdos, Luochuan, Linfen and Yantai); CO_{2ff} in these cities were generally lower than 10 ppm in 2010 (Xi et al., 2013). The likely implication is that cities with large populations have higher CO_2 emissions.

3.5. *The effect of emission sources*

The dominant CO_{2ff} sources in the Xi'an urban district include thermal power plants, vehicle exhaust, and residential emissions. There are two thermal power plants in the investigated area, as shown in Fig. 1: Baqiao Thermal Power Plant (BTPP) in the east, and Western Thermal Power Plant (WTPP) in the west. We found that the CO_{2ff} mixing ratio of the sites in the downwind area (southwest) near BTPP and WTPP, such as Changle Park (CLP), Xingqing Palace Park (XQP) and Epang Palace Relic Park (EPRP), was not especially elevated, when compared to results from the other regions. This might be attributable to enhanced diffusion of exhaust gas during transport from the very high power plant vents to the ground (Zhang, 2013). Our results suggest, therefore, that these two power plants are not primary contributors to CO_{2ff} spatial variation.

Vehicle exhaust and residential emissions are non-point sources of CO_{2ff} emissions. In general, they are widely distributed within the urban area. In addition, vehicle exhaust is a mobile emission source, which is distinct from residential emissions. Nevertheless, both are closely associated with population density. The two sites (CSP and XEP) with the lowest measured CO_{2ff} values were located in an area in the northeast with low population density. In contrast, relatively high CO_{2ff} values were frequently observed in the south of Xi'an, which includes two of six population centers in this district (Mi et al., 2014). The rapid increase of motor vehicles during 2013–14 (from 1.6349 million to 1.9260 million) but overall slow residential population growth (from 5.8060 million to 5.8716 million) suggested that CO_{2ff} increases observed for many sites were likely related to rapidly growing regional traffic conditions. For example, the Ring Road was under construction, with the addition of three tunnels, to improve the traffic in 2013. This project was completed in April 2014, at which point traffic flow increased rapidly. As a result, at sites SWXW and NWXW, adjacent to the Ring Road, the CO_{2ff} mixing ratio rose from ~20 ppm to ~30 ppm.

3.6. *The effect of weather conditions*

Wind speed and wind direction have a strong influence on CO_2 transport and diffusion, which may be reflected in spa-

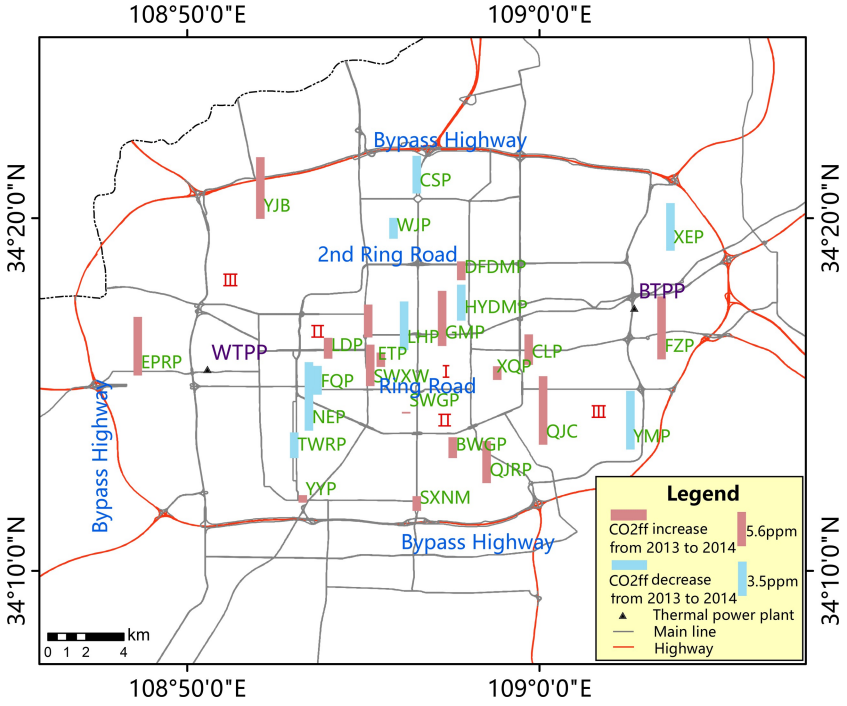

Fig. 4. CO_{2ff} variation from 2013 to 2014. The sites with a CO_{2ff} decrease and increase from 2013 to 2014 are shown in blue and red, respectively.

tial CO_{2ff} variations. The average wind speed during April to September in Xi'an City (Xi'an Jinghe National Meteorological Station, No. 57131) in 2013 and 2014 was 2.66 m s^{-1} and 2.54 m s^{-1}, respectively, with typically low winds of about the same magnitude. Figure 5 shows wind rose diagrams for April to September in 2013 and 2014. The wind differences show an increase in southwesterly winds, and a decrease in north-northeasterly winds in 2014, as compared to 2013. There are some industrial parks in the southwest Xi'an urban area, including the large Xi'an Hi-Tech Industries Development Zone. Emissions from this zone could be carried to urban areas by southwesterly winds (Guo et al., 2014). CO_{2ff} values of most sites near the west and south Bypass Highway did increase from 2013 to 2014, possibly due to more frequent southwesterly winds.

4. Conclusion and perspectives

The spatial distribution of CO_{2ff} indicated by plant $\Delta^{14}C$ measurements in the central Xi'an urban district in the April to September of 2013 and 2014 is presented in this paper. Three characteristics in our observed period based on the above results and discussion are as follows. First, the year-to-year variation of CO_{2ff} from different sites was significant. Second, there was no obvious difference in average CO_{2ff} between the three districts divided by the Ring Road, 2nd Ring Road and the Bypass Highway. Third, the northeast corner of the study area featured distinctly lower CO_{2ff} values than the rest of the sites studied. These spatial and temporal variations were influenced by emission sources and weather conditions. Vehicle exhaust emissions and residential emissions appeared to control the spatial differences. Weather conditions (wind direction in particular) also influenced regional temporal CO_{2ff} variations.

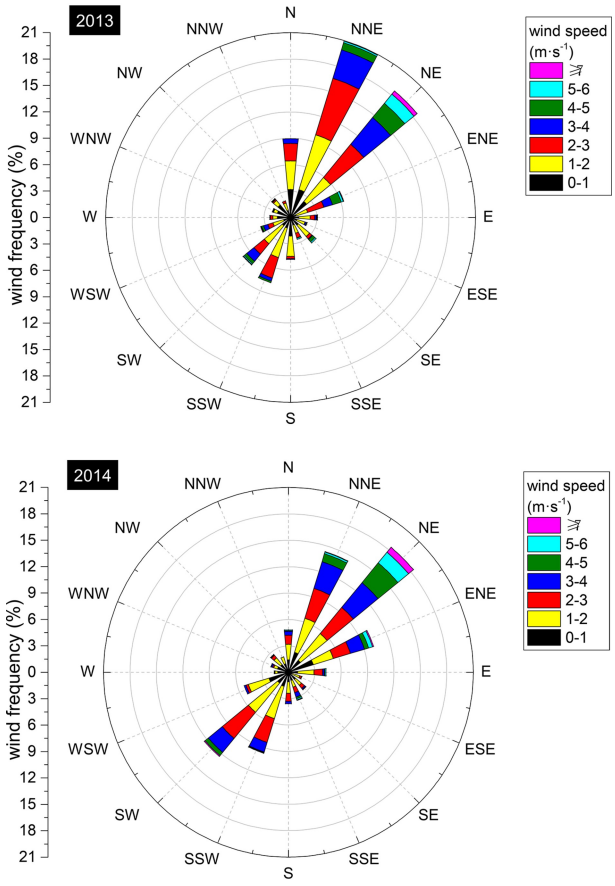

Fig. 5. Wind rose diagrams during April to September in 2013 and 2014. Wind speeds are shown in different colors.

Our results show high spatial and temporal CO_{2ff} variations in Xi'an. Implicit in these results is the need for high spatial resolution, and long-term CO_{2ff} monitoring. To characterize CO_{2ff} spatial distributions in urban areas, plant samples are economical and convenient. To obtain reliable results, there are some recommendations when adopting this method: (a) sampling sites should be chosen carefully, and over a large area, with sites distant from CO_2 emission sources being suitable; (b) the plants should grow in an open environment; and (c) widespread plants with a known growth period are preferable. Such a program would support timely carbon emission reduction measures and efficient policies to cope with future change.

Acknowledgments. The authors would like to thank the anonymous reviewers and Dr. George S. BURR for their helpful comments. This work was jointly supported by the National Natural Science Foundation of China (Grant No. NSFC41730108, 41773141, 41573136, and 41991250), National Research Program for Key Issues in Air Pollution Control (Grant No. DQGG0105-02), the Strategic Priority Research Program of the Chinese Academy of Sciences (Grant No. XDA23010302), the Youth Innovation Promotion Association CAS (Grant No.2016360) and the Natural Science Basic Research Program of Shaanxi (Program No. 2019JCW-20).

REFERENCES

Andres, R. J., and Coauthors, 2012: A synthesis of carbon dioxide emissions from fossil-fuel combustion. *Biogeosciences*, **9**(5), 1845–1871, https://doi.org/10.5194/bg-9-1845-2012.

Beramendi-Orosco, L., and Coauthors, 2015: Temporal and spatial variations of atmospheric radiocarbon in the Mexico City metropolitan area. *Radiocarbon*, **57**(3), 363–375, https://doi.org/10.2458/azu_rc.57.18360.

Bozhinova, D., M. Combe, S. W. L. Palstra, H. A. J. Meijer, M. C. Krol, and W. Peters, 2013: The importance of crop growth modeling to interpret the $\Delta^{14}CO_2$ signature of annual plants. *Global Biogeochemical Cycles*, **27**(3), 792–803, https://doi.org/10.1002/gbc.20065.

Bozhinova, D., S. W. L. Palstra, M. K. van der Molen, M. C. Krol, H. A. J. Meijer, and W. Peters, 2016: Three years of $\Delta^{14}CO_2$ observations from maize leaves in the Netherlands and Western Europe. *Radiocarbon*, **58**(3), 459–478, https://doi.org/10.1017/RDC.2016.20.

Buchwitz, M., and Coauthors, 2017: Global satellite observations of column-averaged carbon dioxide and methane: The GHG-CCI XCO_2 and XCH_4 CRDP3 data set. *Remote Sensing of Environment*, **203**, 276–295, https://doi.org/10.1016/j.rse.2016.12.027.

Djuricin, S., X. M. Xu, and D. E. Pataki, 2012: The radiocarbon

composition of tree rings as a tracer of local fossil fuel emissions in the Los Angeles basin: 1980–2008. *J. Geophys. Res.*, **117**(D12), D12302, https://doi.org/10.1029/2011JD017284.

Guo, W., Y. Cheng, W. Fan, N. Wang, and B. Xiao, 2014: Characteristics and affecting factors of atmospheric pollutants in Xi'an. *Journal of Earth Environment*, **5**(4), 235–242, https://doi.org/10.7515/JEE201404001.(inChinesewithEnglishabstract). (in Chinese with English abstract)

Gurney, K. R., D. L. Mendoza, Y. Y. Zhou, M. L. Fischer, C. C. Miller, S. Geethakumar, and S. de la Rue du Can, 2009: High resolution fossil fuel combustion CO_2 emission fluxes for the United States. *Environmental Science & Technology*, **43**(14), 5535–5541, https://doi.org/10.1021/es900806c.

Hammer, S., and I. Levin, 2017: Monthly mean atmospheric $D^{14}CO_2$ at Jungfraujoch and Schauinsland from 1986 to 2016. *Tellus B*, **65**, 20092, https://doi.org/10.11588/data/10100.

Hoornweg, D., L. Sugar, and C. L. Trejos Gómez, 2011: Cities and greenhouse gas emissions: Moving forward. *Environment and Urbanization*, **23**(1), 207–227, https://doi.org/10.1177/0956247810392270.

Hsueh, D. Y., N. Y. Krakauer, J. T. Randerson, X. M. Xu, S. E. Trumbore, and J. R. Southon, 2007: Regional patterns of radiocarbon and fossil fuel-derived CO_2 in surface air across North America. *Geophys. Res. Lett.*, **34**(2), L02816, https://doi.org/10.1029/2006GL027032.

IPCC, 2006: 2006 *IPCC Guidelines for National Greenhouse Gas Inventories*. IPCC, 1989 pp.

IPCC, 2018: Summary for policymakers. *Global Warming of* 1.5°C. *An IPCC Special Report on the Impacts of Global Warming of* 1.5°C *Above Pre-Industrial Levels and Related Global Greenhouse Gas Emission Pathways, in the Context of Strengthening the Global Response to the Threat of Climate Change, Sustainable Development, and Efforts to Eradicate Poverty*, V. Masson-Delmotte et al., Eds., World Meteorological Organization, 32 pp.

Levin, I., B. Kromer, M. Schmidt, and H. Sartorius, 2003: A novel approach for independent budgeting of fossil fuel CO_2 over Europe by $^{14}CO_2$ observations. *Geophys. Res. Lett.*, **30**(23), 2194, https://doi.org/10.1029/2003GL018477.

Lichtfouse, E., M. Lichtfouse, M. Kashgarian, and R. Bol, 2005: ^{14}C of grasses as an indicator of fossil fuel CO_2 pollution. *Environmental Chemistry Letters*, **3**(2), 78–81, https://doi.org/10.1007/s10311-005-0100-4.

Liu, Z., and Coauthors, 2015: Reduced carbon emission estimates from fossil fuel combustion and cement production in China. *Nature*, **524**, 335–338, https://doi.org/10.1038/nature14677.

Mi, R. H., and Y. Shi, 2014: Identifying method of CBD and sub-CBD based on the distribution of resident population—A case study of Xi'an City. *Journal of Shaanxi Normal University* (*Natural Science Edition*), **42**(3), 97–102, https://doi.org/10.15983/j.cnki.jsnu.2014.03.022. (in Chinese with English abstract)

Nisbet, E., and R. Weiss, 2010: Top-down versus bottom-up. *Science*, **328**(5983), 1241–1243, https://doi.org/10.1126/science.1189936.

Niu, Z. C., and Coauthors, 2016: The spatial distribution of fossil fuel CO_2 traced by $\Delta^{14}C$ in the leaves of gingko (*Ginkgo biloba* L) in Beijing City, China. *Environmental Science and Pollution Research*, **23**(1), 556–562, https://doi.org/10.1007/s11356-015-5211-2.

Peylin, P., and Coauthors, 2011: Importance of fossil fuel emission uncertainties over Europe for CO_2 modeling: Model intercomparison. *Atmospheric Chemistry and Physics*, **11**(13), 6607–6622, https://doi.org/10.5194/acp-11-6607-2011.

Riley, W. J., D. Y. Hsueh, J. T. Randerson, M. L. Fischer, J. G. Hatch, D. E. Pataki, W. Wang, and M. L. Goulden, 2008: Where do fossil fuel carbon dioxide emissions from California go? An analysis based on radiocarbon observations and an atmospheric transport model *J. Geophys. Res.*, **113**, G04002, https://doi.org/10.1029/2007JG000625.

Rosenzweig, C., W. Solecki, S. A. Hammer, and S. Mehrotra, 2010: Cities lead the way in climate-change action. *Nature*, **467**(7318), 909–911, https://doi.org/10.1038/467909a.

Stuiver, M., and H. A. Polach, 1977: Discussion reporting of ^{14}C data. *Radiocarbon*, **19**(3), 355–363, https://doi.org/10.1017/S0033822200003672.

Tans, P., and R. Keeling, 2019: Open Access Data Source. [Available online from ftp://aftp.cmdl.noaa.gov/products/trends/co2/co2_mm_mlo.txt]

Turnbull, J. C., and Coauthors, 2011: Assessment of fossil fuel carbon dioxide and other anthropogenic trace gas emissions from airborne measurements over Sacramento, California in spring 2009. *Atmospheric Chemistry and Physics*, **11**(2), 705–721, https://doi.org/10.5194/acp-11-705-2011.

Turnbull, J. C., and Coauthors, 2015: Toward quantification and source sector identification of fossil fuel CO_2 emissions from an urban area: Results from the INFLUX experiment. *J. Geophys. Res.*, **120**(1), 292–312, https://doi.org/10.1002/2014JD022555.

Turnbull, J. C., E. D. Keller, T. Baisden, G. Brailsford, T. Bromley, M. Norris, and A. Zondervan, 2014: Atmospheric measurement of point source fossil CO_2 emissions. *Atmospheric Chemistry and Physics*, **14**(10), 5001–5014, https://doi.org/10.5194/acp-14-5001-2014.

Turnbull, J. C., E. D. Keller, M. W. Norris, and R. M. Wiltshire, 2016: Independent evaluation of point source fossil fuel CO_2 emissions to better than 10%. *Proceedings of the National Academy of Sciences of the United States of America*, **113**(37), 10 287–10 291, https://doi.org/10.1073/pnas.1602824113.

WMO, 2018: WMO Greenhouse Gas Bulletin. [Available online from https://www.met.ie/cms/assets/uploads/2018/11/ghg-bulletin_14_en.pdf]

Xi, X. T., X. F. Ding, D. P. Fu, L. P. Zhou, and K. X. Liu, 2011: Regional $\Delta^{14}C$ patterns and fossil fuel derived CO_2 distribution in the Beijing area using annual plants. *Chinese Science Bulletin*, **56**(16), 1721–1726, https://doi.org/10.1007/s11434-011-4453-8.

Xi, X. T., X. F. Ding, D. P. Fu, L. P. Zhou, and K. X. Liu, 2013: $\Delta^{14}C$ level of annual plants and fossil fuel derived CO_2 distribution across different regions of China. *Nuclear Instruments and Methods in Physics Research Section B: Beam Interactions with Materials and Atoms*, **294**, 515–519, https://doi.org/10.1016/j.nimb.2012.08.032.

Zhang, Y. L., 2013: The research about Xi'an concentrated heating flue gas emission and diffusion. M.S. thesis, Chang'an University, 69 pp. (in Chinese with English abstract)

Zhou, W. J., S. G. Wu, W. W. Huo, X. H. Xiong, P. Cheng, X. F. Lu, X., and Z. C. Niu, 2014: Tracing fossil fuel CO_2 using $\Delta^{14}C$ in Xi'an City, China. *Atmospheric Environment*, **94**, 538–545, https://doi.org/10.1016/j.atmosenv.2014.05.058.